A first-principles potential energy surface for Eley–Rideal reaction dynamics of H atoms on Cu(111)

M. Persson,[a] J. Strömquist, and L. Bengtsson
Department of Applied Physics, Chalmers University of Technology and Göteborg University, S-412 96 Göteborg, Sweden

B. Jackson and D. V. Shalashilin
Department of Chemistry, University of Massachusetts, Amherst, Massachusetts 01003

B. Hammer
Institute of Physics, Aalborg University, Pontoppidanstræde 103, DK-9220 Aalborg Øst, Denmark

(Received 15 June 1998; accepted 23 October 1998)

We have performed first-principles total-energy calculations of low-dimensional sections of the electronically adiabatic potential energy surface (PES) that are relevant for the Eley–Rideal (ER) reaction of H atoms on a rigid Cu(111) surface. These calculations were performed within density-functional theory using a plane-wave and pseudopotential method and the generalized gradient approximation for the exchange-correlation energy. The calculated energy points for various configurations of one and two atoms on the Cu(111) surface were used to construct a model PES that can be used in ER reaction dynamics calculations. © *1999 American Institute of Physics.* [S0021-9606(99)70804-4]

I. INTRODUCTION

During the last few years, we have witnessed a tremendous progress in understanding the detailed mechanisms and pathways behind simple surface reactions.[1,2] This progress has been made possible by recent advances both in experiments and theory. On the experimental side, the development of molecular beam scattering experiments and laser techniques have now reached a stage where it is possible to study reaction probabilities as a function of the state of the reactants and also to interrogate the state of the product.[3] On the theoretical side, the development of the generalized gradient approximation (GGA)[4] for the exchange-correlation functional in density functional theory (DFT) and efficient algorithms for the solution of the Kohn–Sham equations in DFT-GGA based on the plane-wave and pseudopotential method[5] have made it possible to calculate reactive parts of electronically adiabatic potential energy surfaces for simple molecules on surfaces with useful accuracy for reaction dynamics calculations. Another important advance has been the development of pseudospectral methods[6] for the solution of the time-dependent Schrödinger equation. A prerequisite for these total energy and dynamics calculations has been the ever-increasing availability of fast computers with large memory capabilities. A prime example of all this progress is provided by the experimental and theoretical study of the activated dissociation of hydrogen molecules on copper surfaces.[1,7] The dissociation probability has been measured as a function of kinetic energy, vibrational, and rotational states of the molecule.[7,8] These results have been rationalized and understood from quantum and molecular dynamics calculations[1,9–16] using model potential energy surfaces (PESs) that have been constructed from DFT-GGA calculations.[13,17–19] In particular, a few groups have succeeded in performing quantum dynamics calculations of the dissociation dynamics that treat all six degrees of freedom for the molecule.[20–23]

Another example of an interesting surface reaction mechanism that has recently been studied by dynamics measurements and calculations is the Eley–Rideal (ER) reaction pathway in which an incident species reacts directly with an adsorbate to form a product molecule that promptly leaves the surface. Also in this case, hydrogen on copper has become a model system for the study of this reaction. In particular, the molecular beam studies by Rettner and Auerbach[24–27] of the reaction of incident H(D) atoms with a D(H)-covered Cu(111) surface have provided state-resolved product distributions. Several quasiclassical and quantum molecular dynamics calculations of this reaction have been performed using various models of the PES.[28–35] Similar calculations have also been performed by Kratzer and co-workers[36–38] on tungsten and Si surfaces. Much has been learned about the reaction dynamics for hydrogen atoms on copper from these calculations but the construction of the reactive part of these model PESs has so far been semiempirical except for a recent construction of H atoms on a Si(001) surface.[38] Thus, there is a need to perform DFT-GGA calculations of the reactive parts of PES for two H atoms on Cu(111) that are relevant for the ER, which can be used to assess these model PESs. In principle, it is the same six-dimensional PES that governs both the dissociative and the ER reactions but the corresponding reaction pathways probe vastly different parts of the PES.

In this paper, we present results from such first-principles calculations of four two-dimensional sections of the PES that are relevant for the ER reaction of two H atoms

[a]Electronic mail: tfymp@fy.chalmers.se

on Cu(111). One important aim of these calculations besides understanding the topography and assessing previous semiempirical PESs has been the construction of a model PES from the calculated sections of the PES that can be used in reaction dynamics calculation. To this end, we have also performed DFT-GGA calculations for the attractive branch of the potential energy curves of an H atom in four sites on the Cu(111) surface and also for the binding energy curve of the isolated molecule. For a proper treatment of the asymptotic part of the interactions of the H atom in these various situations, we have included spin polarization in these DFT-GGA calculations. Our model PES is based on a corrugated London–Eyring–Polyani–Sato LEPS-PES in which the attractive part of the Morse potential has been modified to give a good representation of the attractive part of the calculated potential energy curves for the H–H and, in particular, the H–Cu interaction. Some of these results for the first-principles PES and a first attempt to construct a corrugated LEPS-PES have been reported elsewhere.[39]

The paper is organized as follows. In Sec. II A, we present some details behind our DFT-GGA calculations with results detailed in Sec. III A. The form of the modified Morse potentials and the corrugated LEPS-PES are both detailed in Sec. II B and contour plots of various sections of this model PES are presented in Sec. III B. In Sec. IV, we discuss the topography of the various sections of the first-principles PES, the quality of the developed model PES, and relate our results to previous semiempirical PESs. Finally, we give some concluding remarks and a summary in Sec. V.

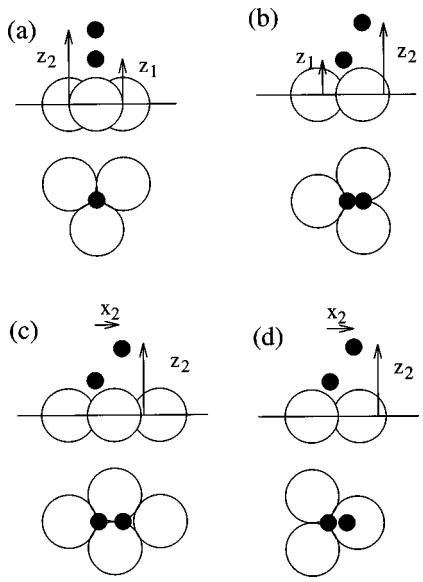

FIG. 1. Definition of the two-dimensional sets of configurations of the two H atoms on the Cu(111) surface: (a) collinear set (*C*), (b) quasicollinear set (QC), (c) hollow-hollow planar set (HHP), (d) hollow-top (HT) set. The H atoms are indicated by small solid circles and the Cu atoms by big open circles. Both a side and a top view of each configuration is displayed. The relevant coordinates are also indicated for each configuration. In (c) and (d) H atom ''1'' is fixed in the chemisorption minimum for a single H atom on Cu(111), that is, the fcc configuration of the hollow site and a distance of about 0.95 Å from the surface plane.

II. THEORY

A. Some details of the total-energy calculations

Our calculations of the total energy for various configurations of one or two H atoms on a Cu(111) surface were based on the density functional scheme using the GGA[4] for the exchange correlation energy. The total energy was computed in a super cell geometry using a plane wave and pseudopotential code.[40] In this code, the Kohn–Sham equations were solved by a combination of a conjugate gradient method[5] and a damped density mixing method.[41]

The first step in the calculations is the definition of the super cell geometry. The Cu(111) surface was represented in the super cell by a slab of four atomic layers in an ABCA stacking and the vacuum region was six layers thick. Each substrate layer contained three Cu atoms and the lattice parameter of the slab was 3.56 Å. The lateral distance between a H atom in the cell and its periodic image is about 4.4 Å. We have considered four sets of configurations of two H atoms and of a single H atom in the cell, respectively. The sets of configurations for the two H atoms are displayed in Fig. 1 and are referred to as the collinear (*C*), quasicollinear (QC), hollow-hollow planar (HHP), and hollow-top planar (HTP) sets. The sets of configurations for the single H atom include the so-called fcc configuration of the hollow site, bridge site, top site, and the site located half way between a top and a hollow site. The various fragment energies such as the total energies of the isolated H atom, H_2 molecule, and Cu(111) surface were obtained from separate calculations in the same super cell.

The form of the pseudopotentials and the size of the plane wave basis set are crucial ingredients of the calculations. The ion cores of the Cu atoms were represented by the fully separable pseudopotential of Troullier and Martins,[42] which includes the $3d$ states as valence states. The hydrogen atom was represented by its bare Coulomb potential. The plane wave set was cut off at a kinetic energy of 50 Ry. The surface Brillouin zone was sampled by 54 special k points with six points in the irreducible wedge for the collinear configurations of two H atoms and for the hollow configurations of a single H atom, whereas the remaining configurations were sampled by 15 points in the irreducible wedge. The present set of computational parameters has been chosen following the findings in Refs. 17 and 13.

In the case of the isolated H atom and the H_2 molecule, we performed some convergence test calculations using plane wave sets up to a cutoff energy of 80 Ry and up to 162 k points. For the standard cutoff of 50 Ry, we find that by enlarging the lateral linear dimensions of the supercell by 50% the total energy of the H_2 molecule changes with less than 0.007 eV. The fact that the interactions between the periodic images of the H_2 molecule are negligible for this larger cell is demonstrated by the result that the total energy of the molecule changes with less than 0.004 eV when using only the Γ point. For the values of 50, 60, 70, and 80 Ry for the cutoff, the calculated energies of the spin-polarized H atom are -13.542, -13.555, -13.572, and -13.584 eV, respectively, and the corresponding potential energies $V_m(r = 0.75\,\text{Å})$ are 4.471, 4.499, 4.508, and 4.516 eV, respec-

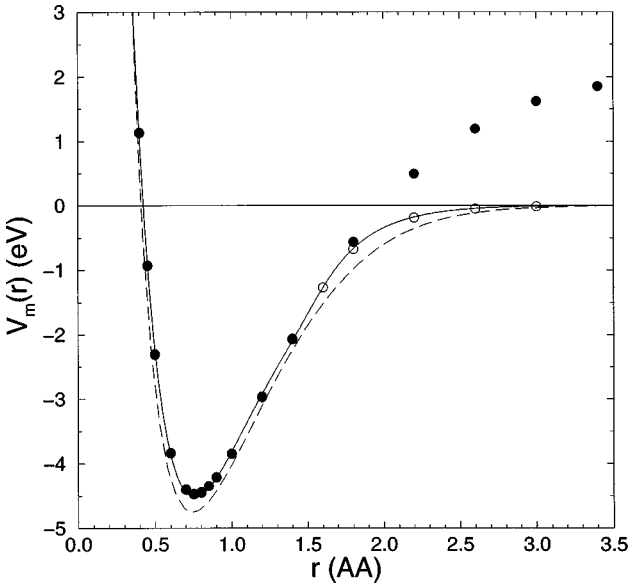

FIG. 2. Calculated potential energy curves for H_2. The potential energies $V_m(r)$ as a function of the interatomic distance, r have been extracted from spin-polarized GGA (open circles) and nonpolarized GGA calculations (solid circles) of the total energy of H_2. $V_m(r)$ is defined in Eq. (3.1). The solid line is the result of a global fit to a modified Morse potential defined in Eq. (2.1) and with parameters tabulated in Table II. The dashed line is the result of an ''exact'' ground state calculation by Kolos and Wolniewicz (Ref. 48).

tively. These values for the H atom are in good agreement with the value of -13.59 eV obtained by Seminario[43] using an extensive atomic-like basis set. Thus, we believe that these calculated energies are well converged.

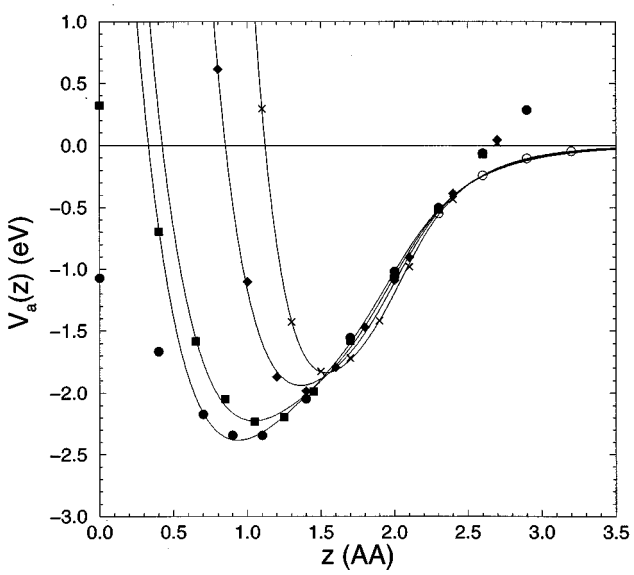

FIG. 3. Calculated potential energy curves for H on various sites of the Cu(111) surface. The potential energy curves $V_a(z)$ for the hollow site (solid circles), bridge site (solid squares), site located half way between hollow and top site (solid diamonds), and top site (crosses) as a function of the distance z have been extracted from GGA post LDA calculations of the total energy of H on Cu(111). The result from spin-polarized GGA calculations for the hollow site is indicated by open circles. $V_a(r)$ is defined in Eq. (3.2). The solid lines are the result of a global fit of the calculated energies to a modified Morse potential defined in Eq. (2.1) and with parameters tabulated in Table II.

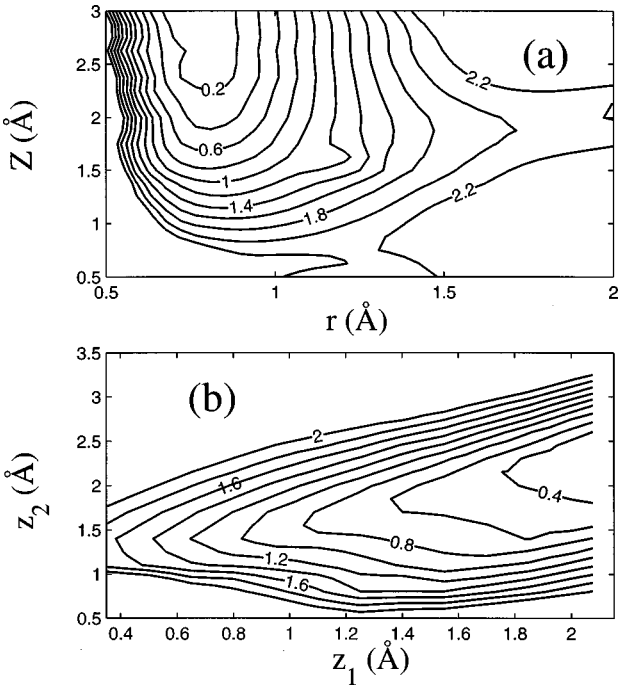

FIG. 4. Contour plot of calculated potential energy surfaces for (a) the collinear and (b) the quasicollinear configurations. These two configurations are defined in Fig. 1: $r=z_2-z_1$ and $Z=(z_1+z_2)/2$. Note that the contour plot in (a) is based on an irregular grid of 100 points, whereas in (b) the grid is regular and contains 56 points. The level spacing is 0.2 eV and the ranges are from 0 to 2.2 eV in (a) and from 0 to 2.0 eV in (b).

To save computer time, we have performed most of the spin-unpolarized calculations in GGA post local density approximation (LDA), that is, self-consistently in the LDA with gradient corrections calculated from the LDA densities using GGA.[4] This approach may in some cases cause problems as discussed by Fuchs and co-workers[44] but in our case there is no such problems for the H atoms because we use the unscreened Coulomb potential and it is not critical for the Cu atoms because the Cu substrate is kept static. All spin-polarized calculations, except some test GGA calculations of the accuracy of GGA post LDA, were performed self-consistently in the GGA. The electronic temperature was 0.1 eV and the energy was extrapolated to zero temperature in a standard manner.[45] Most of the calculations were performed in parallel over k points on the SP2 machine at ''parallel datorcentrum'' (PDC), Stockholm. All our calculated total energies are presented in Figs. 2, 3, 4, and 5.

B. Model potential energy surfaces

The construction of a multidimensional model potential energy surface that can be used in dynamics calculations from the calculated total energies is in general a daunting task and is a subject of current research. Here we have based our construction on a LEPS-like model PES that is both simple and chemically sound. The LEPS-PES was first adapted to reactions at surfaces by McCreery and Wolken[46] and has been widely used.

We have made a modification of the standard LEPS-PES used in surface problems by improving the description of the PES for the fragments. The standard LEPS-PES is based on

a Morse potential for the description of the intramolecular interaction and for the interaction of single atoms with the surface. We have developed a modified Morse potential that gives a much better representation of the attractive branch of these interactions. The generic form of this potential is given by

$$V_\sigma(r)=d_\sigma\{\exp[-2\alpha_\sigma(r-r_{\sigma 0})]-2\,f_\sigma(r)\times\exp[-\alpha_\sigma(r-r_{\sigma 0})]\},\tag{2.1}$$

$$f_\sigma(r)=\exp\left(-\frac{\tilde{\alpha}_\sigma(r-r_{\sigma 0})}{1+\exp[-\beta_\sigma\alpha_\sigma(r-r_{\sigma a})]}\right),\tag{2.2}$$

where $\sigma=a$ or m and corresponds to the single atom surface and the isolated molecule case, respectively. The function $f_\sigma(r)$ contains a switching function in the exponent that causes the exponential decay of the attractive branch to switch from $\exp(-\alpha r)$ to $\exp[-(\alpha+\tilde{\alpha})r]$ in the region around $r_{\sigma a}$. Note that $r_{\sigma 0}$ is close to the position of the potential energy minimum for large values of $\beta_\sigma\alpha_\sigma(r_{\sigma a}-r_{\sigma 0})$.

To account for the surface corrugation of the calculated PES for the single H atom on the Cu(111) surface, we have corrugated the potential parameters of $V_a(r)$ by making an expansion in a Fourier series over surface reciprocal lattice vectors. Using the symmetry of the (111) surface layer, it is possible to group sets of terms in the Fourier series with equivalent coefficients. For instance, in the case of the potential parameter d_a, the resulting expansion is given by

$$d_a(\mathbf{R})=\sum_i d_i h_i(\mathbf{R}).\tag{2.3}$$

For all potential parameters, we have kept the four lowest order terms in this expansion and they are given by

$$\begin{aligned}h_0(\mathbf{R})&=1,\\ h_1(\mathbf{R})&=\cos(2G_0y)+2\cos(G_1x)\cos(G_0y),\\ h_2(\mathbf{R})&=\cos(2G_1x)+2\cos(G_1x)\cos(3G_0y),\\ h_3(\mathbf{R})&=\cos(4G_0y)+2\cos(2G_1x)\cos(2G_0y),\end{aligned}\tag{2.4}$$

where $\mathbf{R}=(x,y)$, the origin is at top site, the x direction is along top site to the bridge site, $G_0=2\pi/(\sqrt{3}a)$, $G_1=\sqrt{3}G_0$, and a is the nearest neighbor distance between two surface atoms. These four terms correspond to 19 terms in the original Fourier series.

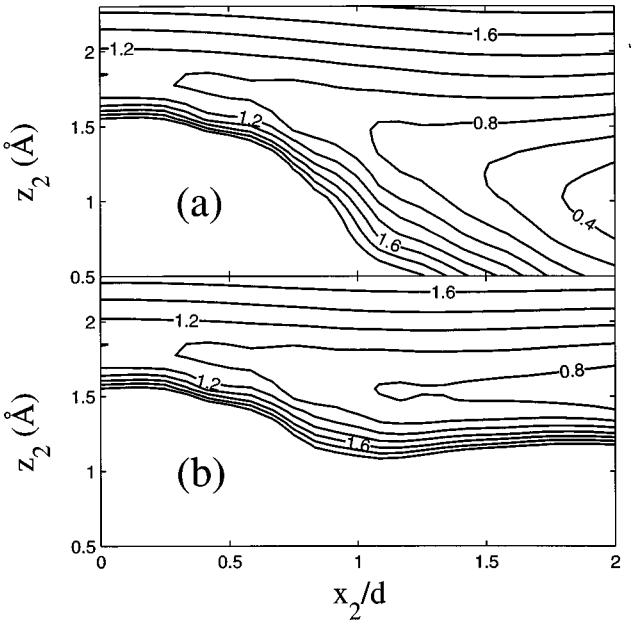

FIG. 5. Contour plot of calculated potential energy surfaces for (a) hollow–hollow and (b) the hollow–top configurations. These two configurations are defined in Fig. 1. d_{HB} is the distance between hollow and bridge site, $d_{\mathrm{HB}}=0.73$ Å. Note that both contour plot are based on regular grids with 42 points in (a) and 37 points in (b). The level spacing is 0.2 eV and the range is from 0 to 2.0 eV in both (a) and (b).

Based on these modified Morse potentials for the fragments, we make an analogous construction of the LEPS-like model PES, $V(\mathbf{r}_1,\mathbf{r}_2)$ as was done for the standard LEPS-PES. In terms of the positions $\mathbf{r}_1$ and $\mathbf{r}_2$ for the two H atoms, this potential is defined as

$$V(\mathbf{r}_1,\mathbf{r}_2)=U_a(\mathbf{r}_1)+U_a(\mathbf{r}_2)+U_m(r)-\sqrt{Q_m(r)^2+[Q_a(\mathbf{r}_1)+Q_a(\mathbf{r}_2)]^2-Q_m(r)[Q_a(\mathbf{r}_1)+Q_a(\mathbf{r}_2)]},\tag{2.5}$$

where $r=|\mathbf{r}_1-\mathbf{r}_2|$. The terms U_σ and Q_σ are now constructed from the repulsive and attractive branches of the modified Morse potential in a manner analogous to the standard LEPS-PES and they are defined as:

$$U_\sigma(r_\sigma)=\frac{1}{4(1+\Delta_\sigma)}d_\sigma\{(3+\Delta_\sigma)\exp[-2\alpha_\sigma(r_\sigma-r_{\sigma 0})]-(2+6\Delta_\sigma)f_\sigma(r_\sigma)\exp[-\alpha_\sigma(r_\sigma-r_{\sigma 0})]\},\tag{2.6}$$

$$Q_\sigma(r_\sigma)=\frac{1}{4(1+\Delta_\sigma)}d_\sigma\{(1+3\Delta_\sigma)\exp[-2\alpha_\sigma(r_\sigma-r_{\sigma 0})]-(6+2\Delta_\sigma)f_\sigma(r_\sigma)\exp[-\alpha_\sigma(r_\sigma-r_{\sigma 0})]\},$$

where $r_m\equiv r$ is the H–H internuclear distance and $r_a\equiv z_1$ or z_2 are the distances of atoms 1 and 2, respectively, above the surface plane. By this construction $V(\mathbf{r}_1,\mathbf{r}_2)$ reduces to modified Morse potentials, Eq. (2.1), for the fragments. When r is large, $V(\mathbf{r}_1,\mathbf{r}_2)$ reduces to $V_a(\mathbf{r}_1)+V_a(\mathbf{r}_2)$, where $V_a=U_a+Q_a$ and it reduces to $V_m(r)=U_m(r)+Q_m(r)$ for large distances z_1 and z_2 from the surface.

III. RESULTS

In this section, we present our calculated results of the total energy for various configurations of two H atoms on a Cu(111) surface, and the construction of a corrugated LEPS-PES from these total energies. An important ingredient in

TABLE I. Calculated and experimental potential energy parameters for an isolated H_2 molecule. $-D_m$ is the energy at the potential energy minimum at r_m and $\hbar\omega_0$ is the vibrational energy in the harmonic approximation. In the present work, these values are based on a quadratic fit to the three lowest energy points. The other calculated values are taken from Perdew *et al.* (Ref. 47) and Seminario (Ref. 43). The ''exact'' values are taken from Kolos and Wolniewicz (Ref. 48).

	D_m (eV)	r_{m0} (Å)	$\hbar\omega_0$ (eV)
Present work	4.48	0.76	0.556
Perdew *et al.*	4.55	⋯	⋯
Seminario	4.78	0.749	⋯
''Exact''	4.748	0.741	0.548

this construction is the results for the total energy of an isolated H_2 molecule and of a single H atom in various sites on the Cu(111) surface.

A. Calculated potential energy surfaces

1. The isolated H_2 molecule

In Fig. 2, we show our calculated potential energy curves $V_m(r)$ for the isolated H_2 molecule as a function of the interatomic distance r. The potential energy $V_m(r)$ is defined as

$$V_m(r)=E_{\mathrm{H-H}}(r)-2E_{\mathrm{H}}, \tag{3.1}$$

where $E_{\mathrm{H-H}}(r)$ is the total energy of the molecule using either spin-polarized or nonpolarized GGA and E_{H} is the total energy of the isolated H atom using spin-polarized GGA. The values that we obtain for the potential energy minimum $-D_m$ and its position r_{m0} and the vibrational energy $\hbar\omega_0$ in the harmonic approximation from a quadratic fit to the three lowest energy points are shown in Table I. The calculations by Seminario[43] and Perdew and co-workers[47] give somewhat differing values for D_m. As shown in Table I, the value from the latter calculation is in good agreement with our calculated value but in comparison with the ''exact'' ground state calculations by Kolos and Wolniewicz[48] our value for D_m is about 5% smaller.

The comparison in Fig. 2 between the results for $V_m(r)$ from spin-polarized and unpolarized calculations demonstrates the importance of including spin polarization to obtain a good description of the dissociation limit. The dissociation energy differs by more than 2 eV in these two cases. In the range $r \gtrsim 1.8$ Å, the inclusion of spin polarization produces a broken symmetry solution in which the orbitals with different spins evolve asymptotically into two separate H $1s$ orbitals. The fact that this solution gives a much better description of the binding energy for H_2 in various local approximations of the exchange-correlation energy in density functional theory is well known and has been widely discussed in the literature.[49] The appearance of spin polarization and its effect on $V_m(r)$ are found to be rather abrupt around $r=1.8$ Å. As shown in Fig. 2, the result for $V_m(r)$ from the ''exact'' ground state calculation[48] shows that this effect on $V_m(r)$ is somewhat more abrupt than the exact $V_m(r)$, and that overall, $V_m(r)$ is relatively well represented by the GGA.

2. A single H atom on Cu(111)

An important region of the interaction of a single H atom with a Cu(111) surface for ER reaction dynamics that has not been studied before by total energy calculations is the region well outside the local potential energy minimum. In Fig. 3 we show the calculated energy curves $V_a(z)$ for a single H atom in four different sites on Cu(111) as a function of the distance z from the surface layer that includes this asymptotic region. This potential energy is defined as

$$V_a(z)=E_{\mathrm{H/Cu}}(z)-E_{\mathrm{H}}-E_{\mathrm{Cu}}, \tag{3.2}$$

where $E_{\mathrm{H/Cu}}(z)$ is the total energy of the H atom on the Cu(111) surface and E_{Cu} is the total energy of the isolated slab. The total energies for the H atom close to the surface and around the equilibrium position are taken from the GGA post LDA calculations by Strömqvist and co-workers,[50] and the total energies for most of the remaining configurations were calculated in this work using GGA post LDA. They noted that fcc and hcp configurations of hollow sites give essentially identical results for the total energies in the region outside the surface. Therefore, we have only shown in Fig. 3 the results for the fcc configuration of the hollow site. As shown in this figure, the calculated $V_a(z)$ in GGA post LDA converges asymptotically to a single potential energy curve but gives the wrong dissociation limit in a similar manner to the isolated hydrogen molecule.

To describe the dissociation limit properly, we have calculated $E_{\mathrm{H/Cu}}(z)$ using spin-polarized GGA in the asymptotic region for the hollow site. The resulting potential energy curve obtained from Eq. (3.2) using the unpolarized GGA value for E_{Cu} and the spin-polarized GGA value for E_{H} is shown in Fig. 3. As expected, this curve shows the proper dissociation limit. We find that the spin polarization starts to notably effect $V_a(z)$ first at $z=2.3$ Å where the net spin (the difference between the number of electrons with spin-up and -down, respectively) is about 0.23. At $z=3.2$ Å where the net spin is about 0.84, we are already very close to the dissociation limit where the net spin is unity for the isolated H atom.

3. Two H atoms on Cu(111)

We have calculated four two-dimensional sections of the potential energy surface that we believe are relevant for the ER reaction of an incident H atom with an adsorbed H atom on Cu(111). The corresponding configurations are displayed in Fig. 1 and are referred to as the C, QC, HHP, and HTP sets.

In Fig. 4(a) we have rendered a contour plot of our calculated potential energies $V(r,z)$ for the set of collinear configurations of two H atoms on Cu(111) as defined in Fig. 1. The relative coordinate r of the two H atoms at distances z_1 and z_2 from the surface plane is defined as $r=z_2-z_1$ and $Z=(z_2+z_1)/2$ is the mid-point coordinate. The potential energy $V(r,z)$ is defined as

$$V(r,z)=E_{\mathrm{H+H/Cu}}(z_1,z_2)-E_{\mathrm{H-H}}(r_{m0})-E_{\mathrm{Cu}}, \tag{3.3}$$

where $E_{\mathrm{H+H/Cu}}(z_1,z_2)$, $E_{\mathrm{H-H}}$, and E_{Cu} are the calculated total energies for the two H atoms on the Cu(111) slab, the isolated H_2 molecule at the potential energy minimum, and

TABLE II. Modified Morse potential energy parameters as extracted from the DFT-GGA calculations. All these parameters were obtained by a least square fit of the modified. Morse potential, Eqs. (2.1) and (2.2), to potential energy curves calculated using DFT-GGA. For the molecule, the range of calculated interatomic distances was from 0.4 to 3 Å. For hollow and bridge sites the fits were limited to the region 0.4 Å outside the surface plane. In all cases, the potential parameter $\beta_\sigma=4$. The errors in the rms sense are also indicated in eV. The units are eV for d_σ and Å for $r_{\sigma 0}$ and $r_{\sigma a}$ and Å^{-1} for α_σ and $\tilde{\alpha}_\sigma$.

σ	d_σ	$r_{\sigma 0}$	α_σ	$\tilde{\alpha}_\sigma$	$r_{\sigma a}$	rms
m	4.505	0.754	2.11	1.1507	1.5	0.0020
a:hollow	2.334	0.916	1.189	1.1337	1.9	0.0011
a:bridge	2.155	1.013	1.180	1.2442	1.92	0.0017
a:top	1.775	1.517	1.758	1.0632	2.0	0.0001
a:hollow/top	1.862	1.335	1.44	1.1322	1.95	0.0016

the isolated Cu(111) slab, respectively. These total energy terms have been generated from both (unpolarized) GGA post LDA and spin-polarized GGA calculations depending on the region of coordinate space. In the region $r \lesssim 1.4$ Å, we find no spin polarization and the calculations of the various total energy terms in Eq. (3.3) are based on GGA post LDA. For a few of these configurations, we have also performed GGA calculations to test the accuracy of GGA post LDA calculations and we find typically a minor difference about 0.03 eV for $V(r,z)$ between GGA post LDA and GGA.

In the region $r \gtrsim 1.4$ Å, we find that a spin-polarized solution of GGA gives a lower $E_{\text{H+H/Cu}}$ than the nonpolarized solution. The former solution has a net spin polarization which rapidly goes to unity for increasing r corresponding to a spin-polarized H atom in the region where no appreciable spin polarization of the other H atom is expected (i.e. $z_1 \lesssim 2.3$ Å). The energy $E_{\text{H+H/Cu}}(z_1,z_2)$ of this solution also goes rapidly to the correct dissociation limit: $E_{\text{H+H/Cu}} \rightarrow E_{\text{H/Cu}}+E_{\text{H}}$. We find that our calculated value of 2.09 eV for the potential energy release

$$\Delta V = V(z_1 = r_{a0}, z_2 \rightarrow \infty) \tag{3.4}$$

is close to the value of 2.11 eV obtained for the sum of the fragment energies $E_{\text{H/Cu}}(r_{a0}) - E_{\text{H}} - E_{\text{Cu}}$ in GGA post LDA. Note that an unpolarized GGA calculation of $E_{\text{H+H/Cu}}$ gives a value for ΔV that would be about 1 eV larger than in spin-polarized GGA.

For the remaining three sets of configurations, all configurations are located in a region, $r \lesssim 1.5$ Å or z_1 and $z_2 \lesssim 2.3$ Å, where the effects of any spin polarization on the energy are negligible. The potential energy of a configuration in any of these three sets has been defined in the same manner as for the collinear set in Eq. (3.3) and all total energy terms have been calculated using GGA post LDA. The contour plot of the potential energy of the quasicollinear configuration has been rendered in Fig. 4(b), whereas the contour plots of the PES for the hollow–hollow and the hollow–top planar configurations have been rendered in Figs. 5(a) and 5(b), respectively.

B. Construction of a model potential energy surface

The construction of our model PES from the first-principles PES for the various configurations of a single H atom and two H atoms on Cu(111) is based on the corrugated LEPS-PES defined in Sec. II B. This model PES is based on modified Morse potentials for the isolated molecule and the single H atom on Cu(111).

As shown in Figs. 2 and 3 the modified Morse potential, defined in Eq. (2.1), gives an excellent fit both to the calculated $V_m(r)$ for the isolated H_2 molecule and to the calculated $V_a(z)$ for the single H atom in the four sites on the Cu(111) surface. As shown in Table II, the root-mean-square (rms) error is typically at most 2 meV. All the deduced potential parameters are also shown in Table II. Note that in our fit to the hollow and the bridge sites we have closed the subsurface absorption channel by excluding the points in the region $z \lesssim 0.4$ Å. In the asymptotic region where the total energy calculations for the hollow site show that spin polarization is important, we have fitted this asymptotic branch for all sites. The four coefficients in the expansion, Eq. (2.3), of the potential parameters for $V_a(z)$ are uniquely determined from the four sites by a linear transformation.

We have determined the Sato parameters, Δ_a and Δ_m defined in Eq. (2.6) by a least square fit of our model LEPS-PES, to be the calculated energy points for the four two-dimensional sections of $V(\mathbf{r}_1,\mathbf{r}_2)$. The resulting values for Δ_a and Δ_m are shown in Table III. The values for the Sato parameters that we use in our construction are obtained from a global fit to all four sets of energy points and are also tabulated in Table III. In Figs. 6 and 7, we have rendered contour plots of the resulting model PES. We will discuss the quality of this PES in Sec. IV.

TABLE III. Sato parameters of the modified and corrugated LEPS-PES. These parameters were determined by a least square fit of the LEPS-PES to the two-dimensional discrete sets of energy points as calculated by DFT-GGA for the configurations defined in Fig. 1. The rms errors are also indicated. The results from a global fit to all sets are also included. The values within the parenthesis refer to the rms error for each set using the Sato parameters obtained from the global fit.

Sets	Δ_a	Δ_m	rms (eV)
C	0.031	−0.075	0.20 (0.20)
QC	0.023	−0.116	0.15 (0.15)
HHP	−0.015	−0.095	0.14 (0.15)
HTP	−0.022	−0.073	0.08 (0.09)
Global	0.02	−0.10	0.16

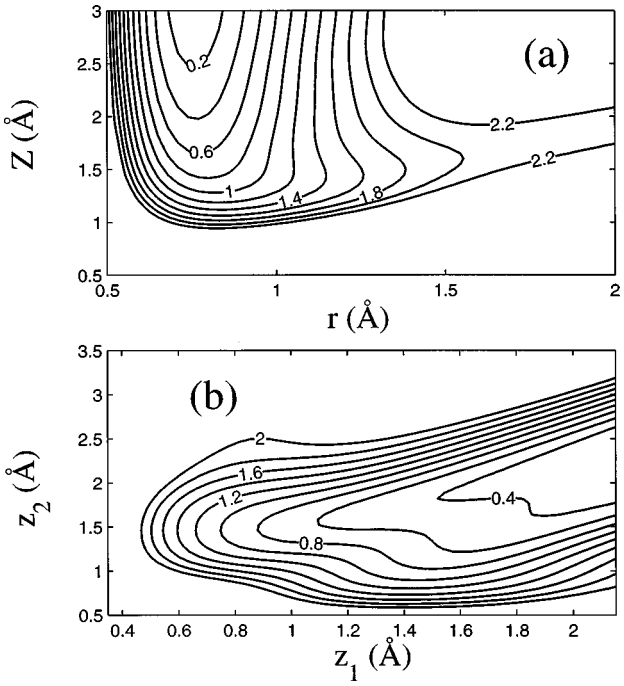

FIG. 6. Contour plots of the corrugated LEPS potential energy surfaces for (a) the collinear and (b) the quasicollinear configurations. The configurations are the same as rendered in Fig. 4 and use the same coordinates. The corrugated LEPS potential energy surface is defined in Sec. II B and its parameters are tabulated in Tables II and III. The level spacing is 0.2 eV and the range is from 0 to 2.2 eV in (a) and from 0 to 2.0 eV in (b).

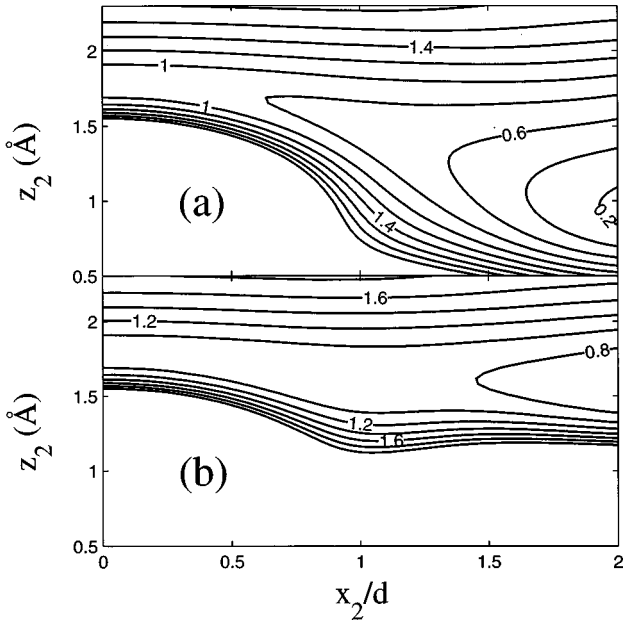

FIG. 7. Contour plots of the corrugated LEPS potential energy surfaces for (a) hollow–hollow and (b) hollow–top configurations. The configurations are the same as rendered in Fig. 5 and use the same coordinates. The corrugated LEPS potential energy surface is defined in Sec. II B and its parameters are tabulated in Tables II and III. The level spacing is 0.2 eV and the range is from 0 to 2.0 eV in both (a) and (b).

IV. DISCUSSION

In this section, we discuss the topography of the sections of the first-principles PES, which all are relevant for the ER reaction of H atoms on Cu(111), and the quality of the developed model PES. Previous semiempirical models of PESs for this ER reaction are also discussed in relation to our first-principles PES.

The overall topography of the four two-dimensional sections of the first-principles PES is relatively simple. The *C* and QC sections of the PES in Fig. 4 show that there is no barrier for the ER reaction of an incident H atom with the adsorbed H atom. These sections exhibit the characteristic feature of an attractive PES, a notion introduced by Polyani in his classical work:[51] a large fraction of the potential energy release is located in the entrance channel. A natural configuration for the measure of the potential energy release in the entrance channel of the *C* section is provided by the configuration $r=r_m$ and $z_1=z_{\mathrm{eq}}$ in which atom 1 is located at the equilibrium position for a single H atom on the surface and the distance between atom 2 and 1 is the same as the equilibrium distance of H_2. The potential energy of this configuration is about 1 eV, which is about 50% of the total potential energy release ΔV of about 2.1 eV. An interesting feature of the *C* section is the presence of a transition state for subsurface absorption in which H atom 1 is located at the surface plane, $z_1=0.0$ Å and H atom 2 is located a distance of about 1.25 Å from the surface plane.

An idea of the behavior of the entrance channel is provided by the HHP and HTP sections of the PES in Fig. 5, in which atom 1 is located at the chemisorption minimum in the hollow site. These sections show that the incident H atom is attracted to the adsorbed H atom but switches to a repulsive interaction between two adsorbed H atoms. For instance, in the one-dimensional manifold of collinear configurations, $x_2=0.0$, the configuration $r=r_m$ and $z=z_{\mathrm{eq}}$ is very close to local minimum but this configuration is a saddle point because it is a local maximum for the lateral motion of the incident H atom. The HHP and HTP sections of the PES also show that the effect of the surface corrugation starts to show up first at lateral distances of about the hollow-bridge distance—that is—~0.7 Å.

A qualitative understanding of the topography of the calculated *C* section of the PES can be obtained from a scrutiny of the calculated electron density rearrangements in space. In Fig. 8 we have rendered such electron densities $\Delta n(\mathbf{x})$ for a few characteristic configurations. The density $\Delta n(\mathbf{x})$ is defined as

$$\Delta n(\mathbf{x})=n_{\mathrm{H+H/Cu}}(\mathbf{x})-n_{\mathrm{Cu}}(\mathbf{x})-\sum_i n_i(\mathbf{x}), \tag{4.1}$$

where $n_{\mathrm{H+H/Cu}}(\mathbf{x})$ is the total electron density, $n_{\mathrm{Cu}}(\mathbf{x})$ is the electron density of the bare Cu slab, and $n_i(\mathbf{x})$ is the electron density of an isolated H atom at the position of atom *i*. First we examine $\Delta n(\mathbf{x})$ in panel (a) of Fig. 8 for the configuration of a single H atom at the equilibrium position in the hollow (fcc) site. The formation of a bond between the H atom and the Cu surface is clearly seen in the increase of $\Delta n(\mathbf{x})$ in this region. As can be seen from the charge arrangements around the surface Cu atom, the Cu *d* states are also strongly involved in this bond. Panels (b) and (c) of Fig. 8 show the charge rearrangements in the presence of a second approaching H atom. As shown in panel (b) already at a

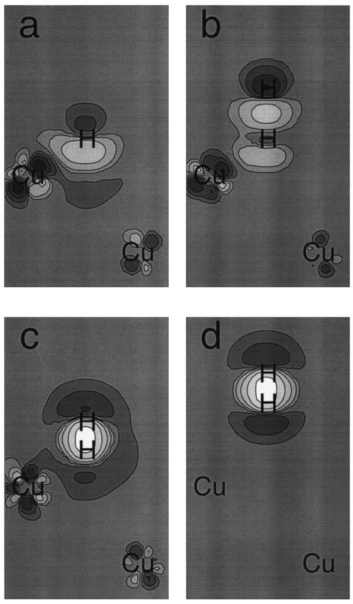

FIG. 8. Contour plots of electron density rearrangements $\Delta n(\mathbf{x})$ for some selected configurations of the collinear section of the PES: (a) a single H atom at the equilibrium position $z_1=0.95$ Å from the surface, (b) a second H atom at the position $z_2=2.3$ Å from the surface, (c) a second H atom at the position $z_2=1.7$ Å from the surface, and (d) an H_2 molecule with interatomic distance 0.8 Å and a center-of-mass distance 2.6 Å from the surface. The lighter and darker contours than the grey background correspond to an increase and a decrease of the electron density, respectively. The scale of the absolute density is logarithmic.

relatively large distance of 1.35 Å a bond charge is built up between the two atoms at the expense of the bond charge between H atom 1 and the surface. This results in an attractive interaction between the H atom and a weakening of the H-surface bond. This behavior is not unexpected for an incoming radical atom such as the open shell H atom and explains why the PES is attractive in the entrance channel. At a closer H–H distance of 0.75 Å a localized bonding charge is built up between the two H atoms. An inspection of the one-electron energy structure shows that this charge is created by filling two electrons into a localized state well below the *d* band. This bonding charge distribution is already similar to the molecular bonding charge distribution, as can be seen from a comparison with the result in panel (d) where the center-of-mass distance is 2.6 Å and the interatomic distance is 0.8 Å. This closed shell results in a repulsive interaction of the H_2 molecule with the surface from the orthogonalization of the metal orbitals to this molecular orbital. Thus this behavior explains the repulsion in the exit channel of the *C* section of the PES.

The presence of a subsurface absorption channel in section *C* of the PES is related to the direct subsurface absorption channel for the PES of a single H atom on Cu(111). As shown in Fig. 3 and as first reported by Strömqvist and co-workers,[50] there is no energy barrier for an H atom incident from the vacuum side to cross the surface plane in the vicinity of the hollow site. The minimum potential barrier is about 1.3 eV above the chemisorption minimum and is about 1.1 eV below the vacuum energy. They found that this barrier drops down by about 0.4 eV when allowing for relaxation of the positions of the substrate atoms. The transition state for the subsurface channel in section *C* of the PES is about 0.1 eV below the chemisorption minimum and shows that the incident H atom promotes absorption of the adsorbed H atom. However, this absorption channel is located away from the minimum energy path from the reactants to the product, which suggests that it might be difficult to access. Note that the subsurface absorption barrier increases rapidly for smaller *r* because a molecular bond is formed between the H atoms, which results in a repulsive interaction with the Cu surface. The presence of this transition state shows also that the reverse process, the recombination of a subsurface H atom with an adsorbed H atom on the rigid surface, has the lowest barrier when the adsorbed atom is displaced about 0.3 Å from its equilibrium position towards the vacuum region. We find that the recombination results in a potential energy release that is almost as large as for the ER reaction. However, for a proper description of these subsurface processes, it is necessary to perform total energy calculations that relax the positions of the substrate atoms. A similar process for the recombination of an adsorbed CH_3 radical on Ni(111) with an absorbed H atom has been identified experimentally by Ceyer and co-workers.[52]

It is not possible to make a direct comparison of the first-principles sections of the PES for the interaction of two H atoms on the Cu(111) with experiments. However, there are two features of the PES for which we can make contact with the experiments. First, the potential energy release ΔV of the ER reaction is related to the maximum internal energy $E_{\max}$ of the product molecule $E_{\max}=\Delta V+E_0+K_i$, where E_0 is the zero-point energy of the adsorbed atom, and K_i is the energy of the incident atom. Rettner and Auerbach[25] find from their state resolved molecular beam experiments that $E_{\max}$ is about 2.5 eV for HD molecules (including the zero-point energy of about 0.23 eV) that are formed in an ER reaction of an incident D beam with adsorbed H atoms on Cu(111). In this experiment, $K_i=0.07$ eV and E_0 is estimated from an analysis based on the harmonic approximation of the measured vibrational energies of the adsorbed H atom by Lamont and co-workers[53] to be about 0.16 eV. From these values, we find that ΔV is about 2.3 eV which is close to the calculated value of 2.1 eV. Second, the PES shows that the interaction between adsorbed H atoms is repulsive, which is consistent with the observation that the maximum stable coverage of H on Cu(111) is at most 2/3. We find that the repulsive interactions between H atoms in neighboring hollow and bridge local minimum sites and in neighboring hollow and hollow local minimum sites are about 1.6 and 0.5 eV, respectively.

Our model PES, based on a corrugated LEPS-PES, gives an excellent representation of the topography of the four sections of the first-principles PES. A direct comparison of the *C* and QC sections of the first-principles and our model PES in Figs. 4 and 6, respectively, shows that these two PESs look very similar except for the subsurface channel in the *C* section. In the construction of the model PES, we have ignored this channel in the PES for a single atom on the Cu(111) surface. As shown in Fig. 3, this latter PES is strictly repulsive close to the surface for all four sites. This

enforced repulsive branch for the H–Cu interaction makes the *C* and QC sections of the model PES more repulsive in the region where atom 1 comes close to the surface plane than in the first-principles PES. As can be seen from Table III, the least squares fit to each set of calculated energy points gives similar values for the Sato parameters and rms errors. This result gives us some confidence that our chosen form of model potential energy surface is appropriate. In a recent paper,[39] we made a preliminary construction of a corrugated LEPS-PES from the four calculated sections of the first-principles PES. An important difference between this model PES and the present one is that the previous model PES was based on Morse potentials for the representation of the H–H and H–Cu(111) interactions. In particular, we find from our new calculations that this representation of the attractive branch of the H–Cu interaction is poor and results in a corrugated LEPS-PES that is too long ranged in the entrance channel. In the present version of the corrugated LEPS-PES, we have used a modified Morse potential that gives a much improved description of this branch of the H–Cu interaction and results in a better description of the entrance channel for the *C* and QC sections and also for the HHP and HTP sections of the first-principles PES. Thus, we believe from this overall comparison that our developed model PES gives a sufficiently good representation of the PES that is useful in ER dynamics calculations.

Another indication of the quality of the present PES is provided by considering a two-dimensional section that is relevant for dissociation of the molecule: the potential energy as a function of the center-of-mass distance form the surface and the interatomic distance when the molecule is oriented parallel to surface above the bridge site with the hydrogen atoms pointing towards their chemisorption sites. Our model PES gives a value of 0.54 eV and a position $(r,z)=(1.0, 1.2)$ Å for the activation barrier for dissociation. These values are in excellent agreement with the corresponding first-principles values 0.54 eV and (1.1, 1.2) Å, calculated by Hammer and co-workers[17] for the same set of *k* points.

Finally, we would like to stress that our calculated DFT-GGA PES supports previous semiempirical models of the PES for the ER reaction of two hydrogen atoms on Cu(111). An early attempt by Persson and Jackson[28] was based on a flat-surface approximation—no surface corrugation of the H–Cu interaction. The choice of Morse potential parameters for this interaction was guided by measured values for the H–Cu vibrational frequency and binding energy, and the values for the Morse potential parameters for the isolated hydrogen molecule was based on experiments. The resulting Morse potential for the H–Cu interaction turns out to give a good representation of the first-principles binding energy curve around the chemisorption minimum for the hollow site. The Sato parameters were chosen to reproduce the accepted view of the activation barrier for dissociation being late in the entrance channel with a barrier of about 0.6 eV. The chosen Sato parameters: $\Delta_a=0.2$ and $\Delta_m=-0.2$ are close to the values that we used in our previous construction,[39] $\Delta_a=0.1$ and $\Delta_m=-0.2$, and gives thus a very similar topography of the *C* section. This PES was later refined by corrugating the LEPS potential with a corrugation function for H–Cu Morse potential that was based on the DFT-GGA calculations[50] for H on Cu(111), and the same values were kept for the Sato parameters.[54] A corrugated LEPS-PES was also constructed by Dai and Zhang[12] in their quantum dynamics study of dissociative adsorption of H_2 on Cu(111). Their construction was partly based on the DFT-GGA calculations by Hammer and co-workers[17] but Dai and Zhang were not certain that their choice of parameters was accurate or even consistent without sufficient first-principles data. However, it turns out that their H–Cu potential is very similar to the Morse potentials over hollow, bridge, and top sites that was based on first-principles data[50] and that their values for the Sato parameters, $\Delta_a=0.1$ and $\Delta_m=-0.15$, are close to values used in the LEPS-PES for the ER reaction.[31,39]

V. CONCLUDING REMARKS

We have performed first-principle total energy calculations of low-dimensional sections of the electronically adiabatic PES that are relevant for the ER reaction of H atoms on a rigid Cu(111) surface. In this reaction pathway, an incident H atom reacts directly with an adsorbed H atom to form a H_2 molecule that leaves the surface. These calculations were performed within DFT using a plane-wave and pseudopotential method and the generalized gradient approximation for the exchange-correlation energy. To obtain a proper description of the dissociation limit of the various configurations, we included spin polarization in the calculations for these configurations. The calculated energy points for various configurations of one and two atoms on the Cu(111) surface were used to construct a model PES that can be used in ER reaction dynamics calculations. This PES is based on a LEPS construction in which both the H–Cu(111) interaction and the H–H interactions are represented by modified Morse potentials. The surface corrugation of the former interaction is modeled by a Fourier series expansion of the potential parameters, which were determined from a fit to first-principle total energy curves for the H atom in four different sites. The two remaining Sato parameters of the LEPS-PES describing the interaction between the H atoms in the presence of the surface were determined from a least square fit to the four two-dimensional sections of the first-principle PES.

We find that the overall topography of the four sections of the first-principle PES is relatively simple. There is no barrier for the ER reaction pathway, which has a large potential energy release. In the notion introduced by Polyani, the PES is attractive; that is, a large fraction of the potential energy release is located in the entrance channel. These PES features are in qualitative agreement with the large rovibrational excitation observed for the HD product in molecular beam scattering experiments of H(D) atoms from D(H)-covered surfaces and the calculated energy release is in quantitative agreement with the measured maximum energy of the HD product. The first-principle PES supports qualitatively and even semiquantitatively previous semiempirical PESs constructed for this reaction. One interesting feature of the PES that has not been anticipated by these semiempirical constructions is the presence of a subsurface channel in

which an adsorbed H atom is promoted by the incident H atom to absorb in a subsurface state. This channel is not easily accessed in the ER pathways and in our construction of the model PES, we have ignored this channel. Otherwise our model PES gives an excellent representation of the topography of the first-principle PES, especially in the view of its small number of parameters. In particular, the use of Morse potential with a modified attractive branch gives a better representation of the interaction of the incident H atom with the surface and the adsorbed H atom than in previous models. Thus we believe that our developed model PES gives a sufficiently good representation of the PES to be useful in ER reaction dynamics calculations.

ACKNOWLEDGMENTS

The present work was mainly supported by the Swedish Natural Science Research Council (NFR), the National Board for Industrial and Technical Development (NUTEK), and in part by the Danish Research Councils through the Center for Surface Reactivity and Grant No. 9501775. Allocation of computer resources at the center of parallel computing (PDC) is gratefully acknowledged. Two of the authors (B.J. and D.S.) gratefully acknowledge support from the Division of Chemical Sciences, Office of Basic Energy Sciences, Office of Energy Research, U.S. Department of Energy, under Grant No. DE-FG02-87ER13744.

[1] G. R. Darling and S. Holloway, Rep. Prog. Phys. **58**, 1595 (1995).
[2] C. Rettner, D. J. Auerbach, J. C. Tully, and A. W. Kleyn, J. Phys. Chem. **100**, 13021 (1996).
[3] C. Rettner and M. Ashfold, *Dynamics of Gas-Surface Interactions, Advances in Gas-Phase Photochemistry and Kinetics* (The Royal Society of Chemistry, London, 1991).
[4] J. P. Perdew, J. A. Chevary, S. H. Vosko, K. A. Jackson, M. R. Pederson, D. J. Singh, and C. Fiolhais, Phys. Rev. B **46**, 6671 (1992).
[5] M. C. Payne, M. P. Teter, D. C. Allen, T. A. Anàs, and J. D. Joannopoulos, Rev. Mod. Phys. **64**, 1045 (1992).
[6] C. Cerjan, *Numerical Grid Methods and their Applications to Schrödinger's Equation*, NATO ASI Series C, Vol. 412 (Kluwer Academic, Dordrecht, 1993).
[7] C. T. Rettner and D. J. Auerbach, in *Surface Reactions*, edited by R. J. Madix (Springer, Berlin, 1993), p. 186.
[8] H. Hou, S. J. Guilding, C. T. Rettner, A. M. Wodtke, and D. J. Auerbach, Science **277**, 80 (1997).
[9] G. Darling and S. Holloway, J. Chem. Phys. **101**, 3268 (1994).
[10] J. Sheng and J. Z. H. Zhang, J. Chem. Phys. **99**, 1373 (1993).
[11] J. Dai, J. Sheng, and J. Z. H. Zhang, J. Chem. Phys. **101**, 1555 (1994).
[12] J. Dai and J. Z. H. Zhang, J. Chem. Phys. **102**, 6280 (1995).
[13] A. Gross, B. Hammer, M. Scheffler, and W. Brenig, Phys. Rev. Lett. **73**, 3121 (1994).
[14] A. D. Kinnersley, G. R. Darling, S. Holloway, and B. Hammer, Surf. Sci. **364**, 219 (1996).
[15] G. J. Kroes, G. Weisenekker, E. J. Baerends, R. C. Mowrey, and D. Neuhauser, J. Chem. Phys. **105**, 5979 (1996).
[16] G. J. Kroes, G. Weisenekker, E. J. Baerends, and R. C. Mowrey, Phys. Rev. B **53**, 10397 (1996).
[17] B. Hammer, M. Scheffler, K. Jacobsen, and J. K. Nørskov, Phys. Rev. Lett. **73**, 1400 (1994).
[18] J. White, D. Bird, M. Payne, and I. Stich, Phys. Rev. Lett. **73**, 1404 (1994).
[19] G. Weisenekker, G. J. Kroes, and E. J. Baerends, J. Chem. Phys. **104**, 7344 (1996).
[20] G. J. Kroes, E. J. Baerends, and R. C. Mowrey, Phys. Rev. Lett. **78**, 3583 (1997).
[21] G. J. Kroes, E. J. Baerends, and R. C. Mowrey, J. Chem. Phys. **107**, 3309 (1997).
[22] J. Dai and J. C. Light, J. Chem. Phys. **107**, 1676 (1997).
[23] A. Gross and M. Scheffler, Phys. Rev. B **57**, 2493 (1998).
[24] C. Rettner, Phys. Rev. Lett. **69**, 383 (1992).
[25] C. Rettner and D. Auerbach, Phys. Rev. Lett. **74**, 4551 (1995).
[26] C. T. Rettner and D. J. Auerbach, J. Chem. Phys. **104**, 2732 (1996).
[27] C. T. Rettner and D. J. Auerbach, Surf. Sci. **357/358**, 602 (1996).
[28] B. Jackson and M. Persson, J. Chem. Phys. **96**, 2378 (1992).
[29] B. Jackson and M. Persson, Surf. Sci. **269/270**, 195 (1992).
[30] B. Jackson, M. Persson, and B. D. Kay, J. Chem. Phys. **100**, 7687 (1994).
[31] M. Persson and B. Jackson, J. Chem. Phys. **102**, 1078 (1995).
[32] M. Persson and B. Jackson, Chem. Phys. Lett. **237**, 468 (1995).
[33] B. Jackson and M. Persson, J. Chem. Phys. **103**, 6257 (1995).
[34] B. Jackson and M. Persson, in *Elementary Processes in Excitations and Reactions on Solid Surfaces*, Springer Series in Solid-State Sciences, Vol. 121, edited by A. Okiji, K. Makoshi, and H. Kasai (Springer, Berlin, 1996), p. 26.
[35] P. Kratzer and W. Brenig, Z. Phys. B **99**, 571 (1996).
[36] P. Kratzer and W. Brenig, Surf. Sci. **254**, 275 (1991).
[37] P. Kratzer, J. Chem. Phys. **106**, 6752 (1997).
[38] P. Kratzer, Chem. Phys. Lett. **288**, 336 (1998).
[39] D. V. Shalashilin, B. Jackson, and M. Persson, Faraday Discuss. **110**, 287 (1998).
[40] B. Hammer, *DACAPO version 1.18* (CAMP, Technical University, Denmark).
[41] G. Kresse and J. Forthmüller, Comput. Mater. Sci. **6**, 15 (1996).
[42] N. Troullier and J. L. Martins, Phys. Rev. B **43**, 1993 (1991).
[43] J. M. Seminario, Int. J. Quantum Chem. Symp. **28**, 655 (1994).
[44] M. Fuchs, M. Bockstedte, E. Pehlke, and M. Scheffler, Phys. Rev. B **57**, 2134 (1998).
[45] M. Gillan, J. Phys.: Condens. Matter **1**, 689 (1989).
[46] J. McCreery and G. Wolken Jr., J. Chem. Phys. **63**, 2340 (1975).
[47] J. P. Perdew, K. Burke, and M. Ernzerhof, Phys. Rev. Lett. **77**, 3865 (1996).
[48] W. Kolos and L. Wolniewicz, J. Chem. Phys. **43**, 2429 (1965).
[49] B. I. Dunlap, in *Ab-initio Methods in Quantum Chemistry-II*, edited by K. P. Lawley (Wiley, New York, 1987), p. 287.
[50] J. Strömquist, L. Bengtsson, M. Persson, and B. Hammer, Surf. Sci. **397**, 382 (1998).
[51] J. C. Polyani, Acc. Chem. Res. **5**, 6 (1972).
[52] K. J. Maynard, A. D. Johnson, S. P. Daley, and S. T. Ceyer, Faraday Discuss. Chem. Soc. **91**, 437 (1991).
[53] C. L. Lamont, B. N. J. Persson, and G. P. Williams, Chem. Phys. Lett. **243**, 429 (1995).
[54] S. Caratzoulas, B. Jackson, and M. Persson, J. Chem. Phys. **107**, 6420 (1997).